Graphical Models 76 (2014) 289–300

Contents lists available at ScienceDirect

Graphical Models

journal homepage: www.elsevier.com/locate/gmod

Hierarchical B-splines on regular triangular partitions

Hongmei Kang, Falai Chen *, Jiansong Deng

School of Mathematical Sciences, University of Science and Technology of China, Hefei, Anhui 230026, PR China

ARTICLE INFO

Article history:
Available online 4 April 2014

Keywords:
Hierarchical splines
Triangular partition
Multivariate B-splines
Surface fitting
Numerical PDEs

ABSTRACT

Multivariate splines have a wide range of applications in function approximation, finite element analysis and geometric modeling. They have been extensively studied in the last several decades, and specially the theory on bivariate B-splines over regular triangular partition is well developed. However, the above mentioned splines do not have local refinement property – a property that is very important in adaptive function approximation and level of detailed representation of geometric models. In this paper, we introduce the concept of hierarchial bivariate splines over regular triangular partitions and construct basis functions of such spline space that satisfy some nice properties. We provide some examples of hierarchical splines over triangular partitions in surface fitting and in solving numerical PDEs, and the results turn out to be promising.

1. Introduction

In CAD/CAM industry, free form surfaces are usually represented by tensor product polynomials or rational maps, such as tensor-product B-splines and NURBS. For these standard tensor-product representations, local adaptive refinement is naturally supported by the hierarchical spline model, where different levels of details are identified by means of a hierarchy of tensor-product splines [1]. Based on such hierarchical model, complex surfaces can be created from simple NURBS surfaces with hierarchical editing.

Compared to tensor-product representations, splines on triangular partition have the advantage of flexibility and lower degree with the same continuity. The theory on multivariate splines over triangular partitions has been widely studied in the past several decades, see [2] for a detailed survey. However, for arbitrary triangular partition, the spline space depends on not only the topology but also the geometry of the partition, leading to high cost on computation and difficulties in controlling the spline functions. Thus, instead of working with splines over arbitrary triangulation, we focus our attention on bivariate splines over two regular triangular partitions, called type-I triangular partition and type-II triangular partition respectively. The theory of bivariate splines defined on type-I and type-II triangular partition has been well developed by Renhong Wang et al. [2]. Unfortunately, such kind of splines does not have local refinement property, which limits its applications in Computer Aided Design (CAD) and finite element analysis.

In this paper, we extend the hierarchical representations from tensor-product splines to splines defined on regular triangular partitions. The idea is to define a set of basis functions by certain rules from a sequence of nested bivariate spline spaces defined on a nested regular triangular partition. The refinement domain can be any type which is convenient to capture local details. We call such hierarchial model on regular triangular partition as hierarchical bivariate splines. The functions in such spline space have some nice properties which are useful in finite element analysis and CAD.

2. Related work

To address the problem of local refinement of splines on rectangular domain, the concept of hierarchical B-splines

* Corresponding author.
E-mail address: chenfl@ustc.edu.cn (F. Chen).

http://dx.doi.org/10.1016/j.gmod.2014.03.002
1524-0703/

(HB-splines for short) was firstly introduced by Forsey and Bartels as an accumulation of B-splines with nested knot vectors [1]. HB-splines can be locally refined using overlays. Later researches mainly focus on how to construct bases of hierarchical B-spline spaces. The first specific basis selection mechanism was proposed by Kraft in [3], and extended by Vuong et al. in [4]. The basis functions of the hierarchical spline space constructed in [4] are non-negative, linearly independent and locally supported. Shortly after, Jüttler et al. normalized the hierarchical B-splines proposed in [4] by reducing the support of basis functions defined on coarse grids, according to finer levels in the hierarchy of splines [5]. They call such hierarchical B-splines as truncated hierarchical B-splines (THB-splines), which are non-negative, locally supported, linearly independent and form a partition of unity, and allow an effective local control of refinement.

There are also several other kinds of local refinement splines developed in the past decade besides HB-splines. *T-splines* were introduced by Sederberg et al. as a generalization of NURBS surfaces [6,7]. The control meshes of T-splines permit T-junctions, which allows T-splines locally refinable without propagating entire columns or rows. This property makes T-splines an ideal modeling tool for complicated geometry. However, T-splines blending functions are not always linearly independent, which limits its its applications in analysis. A solution to this problem is the so called *analysis-suitable T-splines* [8] which are a subset of T-splines defined over a restricted T-mesh whose T-junction extensions do not intersect. The blending functions of AST splines are always linearly independent and thus is suitable for finite element analysis. Other types of local refinement splines proposed in recent years include *PHT-splines* [9] and *LR-splines* [10], etc. They also have good properties which are ideal in CAD and iso-geometric analysis, for more details we the reader refer to [9,10].

An attractive alternative of tensor-product representation is to define piecewise polynomials on triangular partitions, since a triangulation has more flexibility to be adapted to arbitrary shapes. Traditional finite element spaces are defined on conforming triangulation, and local refinement must guarantee the conformability of the triangulation. Furthermore, to construct smooth (at least C^1 continuous) finite elements, generally high degree polynomials are required (for example, Argyris element consists of quintic polynomials with C^1 continuity globally) or each triangle is further subdivided into many sub-triangles (e.g., for Powell–Sabin elements, each macro-triangle is subdivided into 6 sub-triangles [11]). Recently, Speleers et al. constructed hierarchical Powell–Sabin splines for iso-geometric analysis applications [12,13]. Another related work is hierarchical triangular splines (HTS) introduced in [14]. A HTS spline surface is a piecewise quintic Bézier surface and is overall tangent plane continuous. The local refinement can be done by splitting each of the refined triangles into four sub-triangles regularly, which is referred to as a macro-patch. The Bézier ordinates on a macro-patch are constrained by G^1 continuity. HTS mainly focuses on modeling instead of analysis.

In this paper, we extend HB-splines paradigm to bivariate splines defined on regular triangulation. Starting from a spline space over a regular triangulation, we construct a nested spline space sequences according to the successive refinements of the regular triangulation by taking a similar approach as in [4]. This construction can be easily generalized to the spline spaces defined on other triangulation if local support basis functions of the space can be constructed. In this paper, we will focus our attention on spline spaces $S_3^1(\Delta_{mn}^{(1)}) - C^1$ continuous cubic splines over type-I triangulations, and $S_2^1(\Delta_{mn}^{(2)}) - C^1$ continuous quadratic splines over type-II triangulations which will be defined in details in Section 3.2.

The remainder of the current paper is organized as follows. In Section 3, we review some preliminary knowledge about bivariate splines defined on type-I or type-II triangular partition. In Section 4, the construction of hierarchical bivariate splines is described. Some properties of hierarchical bivariate spline basis functions are discussed. In Sections 5 and 6, applications of hierarchical bivariate splines in surface fitting and finite element analysis are demonstrated. Section 7 concludes the paper with a summary and future work.

3. Bivariate splines space defined on type-I and type-II triangular partitions

In this section, we recall some preliminary knowledge about bivariate splines defined on type-I and type-II partitions which have been thoroughly discussed in [2]. Without of generality, we assume that the initial domain $D = [0, m] \otimes [0, n]$ is a rectangle domain, here m, n are positive integers. L-type domain can be segmented into several rectangles. We should note that any linear transformation of the domain does not influence the results in this section, so D can be any parallelogram.

3.1. Splines space defined on type-I triangular partition

Type-I triangular partition, denoted by $\Delta_{mn}^{(1)}$, is constructed by connecting the diagonal line segment with positive slope of every rectangular cell of a uniform rectangular partition, see Fig. 1(a):

$$\Delta_{mn}^{(1)} : x = i, y = j,\ x - y = h,$$

where $i = 1, \ldots, m-1,\ j = 1, \ldots, n-1$, and $h = -n+1, \ldots, m-1$.

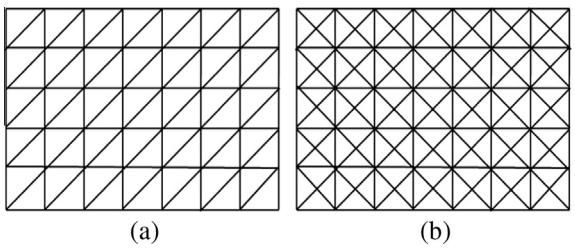

Fig. 1. (a) Type-I triangular partition. (b) Type-II triangular partition.

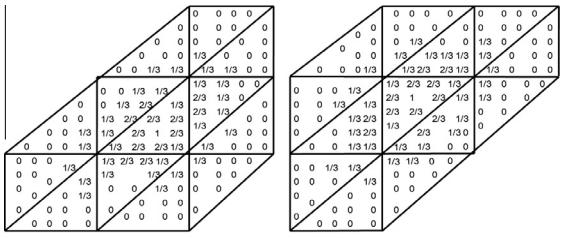

(a) $B^1(x,y)$ (b) $B^2(x,y)$

Fig. 2. Bézier expressions of $B^1(x,y)$ and $B^2(x,y)$ in $S_3^1(\Delta_{mn}^{(1)})$. The numbers in every triangle are the Bézier ordinates.

The spline space defined on a type-I triangular partition is denoted by $S_k^\mu(\Delta_{mn}^{(1)})$, where k and μ are the degree and order of smoothness of the splines respectively.

Proposition 1 [2]. *The dimension of the spline space* $S_k^\mu(\Delta_{mn}^{(1)})$ *is given by*

$$\begin{aligned} dim S_k^\mu(\Delta_{mn}^{(1)}) = &\binom{k+2}{2} + (2m+2n-3)\binom{k-\mu+1}{2} \\ &+ (m-1)(n-1)(k-\mu \\ &-[(\mu+1)/2])_+ \cdot (k-2\mu+[(\mu+1)/2]). \end{aligned} \tag{1}$$

k and μ must satisfy the following inequality

$$k > (3\mu+1)/2,$$

if $S_k^\mu(\Delta_{mn}^{(1)})$ has basis functions with local support. For a given order of smoothness μ, generally it is expected that the degree of the spline function is as low as possible. For example, $S_3^1(\Delta_{mn}^{(1)})$ is the spline space with lowest degree for the given order of smoothness $\mu = 1$.

Now we review the construction of basis functions with local support of spline space $S_3^1(\Delta_{mn}^{(1)})$. $S_3^1(\Delta_{mn}^{(1)})$ is spanned by the translation of two kinds of locally supported functions $B^1(x,y)$ and $B^2(x,y)$, where $B^2(x,y) = B^1(-x,-y)$. That is

$$S_3^1(\Delta_{mn}^{(1)}) = span\{B_{ij}^1 | (i,j) \in Q_1\} \cup \{B_{ij}^2 | (i,j) \in Q_2\},$$

where $B_{ij}^p = B^p(x-i, y-j)$, $Q_p := \{(i,j) | \exists (x,y) \in D,\ s.t. B_{ij}^p(x,y) \neq 0\}$, $p = 1, 2$.

For effective computation, we express $B^1(x,y)$ and $B^2(x,y)$ in the form of Bézier ordinates. Fig. 2 shows the supports together with the Bézier ordinates of $B^1(x,y)$ and $B^2(x,y)$ respectively. Their shapes are depicted in Fig. 3.

Since $\#(Q_1 \cup Q_2) = 2(m+2)(n+2) - 2$ and $dim S_3^1(\Delta_{mn}^{(1)}) = 2(m+2)(n+2) - 5$, the functions in set $\widetilde{\mathfrak{B}} = \{B_{ij}^1 | (i,j) \in Q_1\} \cup \{B_{ij}^2 | (i,j) \in Q_2\}$ are linearly dependent. Fortunately, by removing three functions in $\widetilde{\mathfrak{B}}$, a set of linearly independent basis functions $\mathfrak{B}$ can be obtained which spans $S_3^1(\Delta_{mn}^{(1)})$. $\mathfrak{B}$ is defined as follows

$$\begin{aligned} \mathfrak{B} = \{&B_{ij}^1, B_{ij}^2 | (i,j) \in Q_1(m, n+1), \\ &(s,t) \in Q_2(m+1, n; m+1, n-1)\}, \end{aligned} \tag{2}$$

where $Q_p(i_1, j_1; \ldots; i_q, j_q) = Q_p \backslash \{(i_1, j_1), \ldots, (i_q, j_q)\}$, $p = 1, 2$.

The basis functions in $\mathfrak{B}$ are non-negative, locally supported and $\mathbb{P}_1 \subset S_3^1(\Delta_{mn}^{(1)})$. More precisely, polynomials $1, x, y \in \mathbb{P}_1$ can be represented by linear combinations of basis functions in $\mathfrak{B}$ [2].

3.2. Splines space defined on type-II triangular partition

Type-II triangular partition is constructed by connecting the two diagonal line segments of every rectangular cell of a uniform tensor-product partition, that is, type-II triangular partition $\Delta_{mn}^{(2)}$ is composed of the following lines:

$$x = i, \quad y = j, \quad y - x = h_1, \quad x + y = h_2,$$

where $i = 1, \ldots, m-1, j = 1, \ldots, n-1, h_1 = 1-n, \ldots, m-1, h_2 = 1, \ldots, m+n-1$. See Fig. 1(b) for a reference.

A spline space defined on a type-II triangular partition is denoted by $S_k^\mu(\Delta_{mn}^{(2)})$.

Proposition 2 [2]. *The dimension of* $S_k^\mu(\Delta_{mn}^{(2)})$ *is given by*

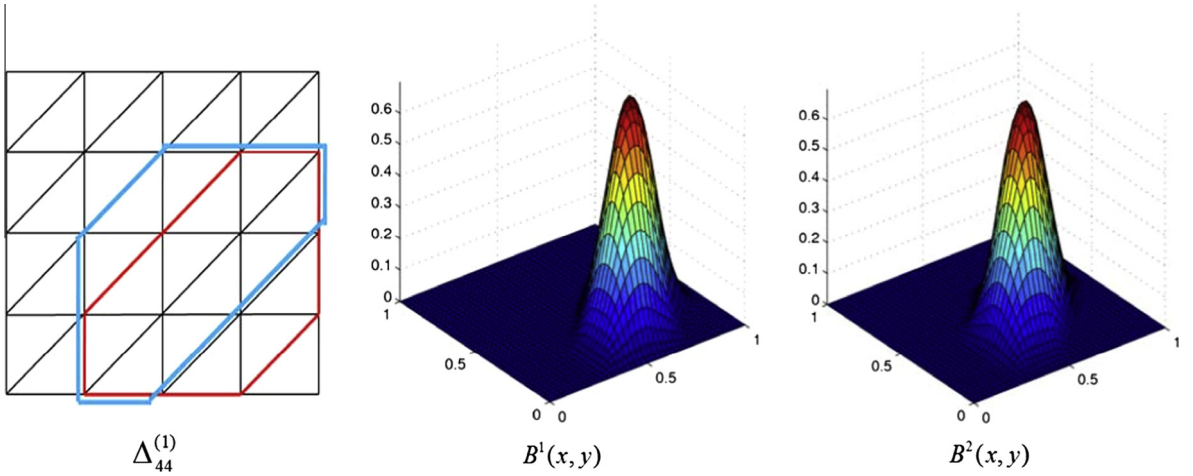

$\Delta_{44}^{(1)}$ $B^1(x,y)$ $B^2(x,y)$

Fig. 3. The left figure is a type-I triangular partition, where the interior of red polygon (blue polygon) is the support of $B^1(x,y)(B^2(x,y))$. The right two figures are the shapes of $B^1(x,y)$ and $B^2(x,y)$ respectively. (For interpretation of the references to color in this figure legend, the reader is referred to the web version of this article.)

$$dimS_k^{\mu}(\Delta_{mn}^{(2)}) = \binom{k+2}{2} + (3m+3n-4)\binom{k-\mu+1}{2} + mn\binom{k-2\mu}{2} + (m-1)(n-1)d_k^{\mu}(4), \tag{3}$$

where $d_k^{\mu}(4) = \frac{1}{2}(k-\mu-[(\mu+1)/3])_+ \cdot (3k-5\mu+3[(\mu+1)/3]+1)$.

k and μ should satisfy the following inequality:

$$k > (4\mu+1)/3,$$

in order to get basis functions with local support. Typical spline spaces interested include $S_2^1(\Delta_{mn}^{(2)})$ and $S_4^2(\Delta_{mn}^{(2)})$.

Now we review the construction of locally supported basis functions of spline space $S_2^1(\Delta_{mn}^{(2)})$.

A basic B-spline basis function $C(x,y)$ in $S_2^1(\Delta_{mn}^{(2)})$ is defined as in Fig. 4(a), where the equilateral octagon Q is the support of $C(x,y)$ and the numbers in a triangle are the Bézier ordinates of $C(x,y)$. Notice that the Bézier ordinates in some triangles are not shown, this is because $C(x,y)$ is x-axial and y-axial symmetry, and also symmetric to the origin, and the Bézier ordinates of $C(x,y)$ on these triangles can be deduced by symmetry. The octagon Q is centered at $(\frac{1}{2},\frac{1}{2})$. Fig. 4(b) illustrates the shape of $C(x,y)$.

The dimension of $S_2^1(\Delta_{mn}^{(2)})$ is $(m+2)(n+2)-1$, and a set of linearly independent basis functions for $S_2^1(\Delta_{mn}^{(2)})$ can be constructed as

$$\mathfrak{B} = \{C_{ij}(x,y) : (i,j) \in E, \quad (i,j) \neq (i_0,j_0)\}, \tag{4}$$

where $C_{ij}(x,y) = C(x-i,y-j)$, $E = \{(i,j) : -1 \leqslant i \leqslant m, -1 \leqslant j \leqslant n\}$ and (i_0,j_0) can be any specified index in E.

A nice property of spline space $S_2^1(\Delta_{mn}^{(2)})$ is polynomial completeness – it contains quadratic polynomial space $\mathbb{P}_2$.

Another spline space with locally supported basis over type-II partition is $S_4^2(\Delta_{mn}^{(2)})$. We omit the detailed construction and refer the reader to [2] for a reference. We should point out that this spline space contains cubic polynomial space $\mathbb{P}_3$.

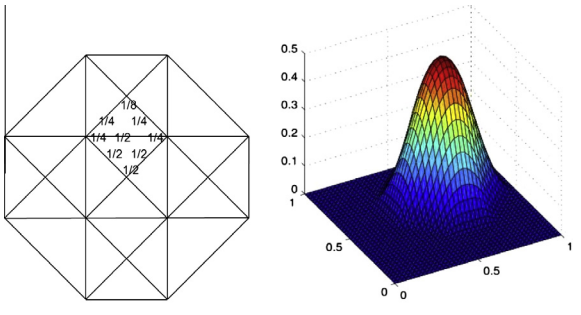

(a) octagon Q (b) function shape

Fig. 4. (a) The Bézier ordinates of $C(x,y) \in S_2^1(\Delta_{mn}^{(2)})$. The Bézier ordinates in other triangles can be deduced by symmetry. (b) The shape of function $C(x,y)$.

4. Construction of hierarchical bivariate splines

In this section, we are going to construction hierarchical bivariate splines over triangular partitions of type-I and type-II. The properties of such hierarchical splines are also presented. For convenience, we use Δ to denote a type-I or type-II triangular partition, and S can be any of spline spaces defined on Δ discussed in the last section. H denotes the corresponding hierarchical spline space defined on a hierarchical triangular partition as explained below.

4.1. Notations

Let

$$S^0 \not\subseteq S^1 \not\subseteq \cdots \not\subseteq S^N,$$

be a nested sequence of bivariate spline spaces defined on a nested sequence of regular triangular partitions of a rectangular domain Ω_0:

$$\Delta^0 \subseteq \Delta^1 \subseteq \cdots \subseteq \Delta^N.$$

Here the notation $\Delta^{k-1} \subseteq \Delta^k$ means Δ^k is a refinement of Δ^{k-1}, that is, Δ^k is obtained by subdividing each cell of Δ^{k-1} into four sub-triangles such that the resulting partition has the same type (type-I or type-II) as Δ^{k-1}. In addition, let

$$\Omega_0 \supseteq \Omega_1 \cdots \supseteq \Omega_N, \Omega_{N+1} = \emptyset,$$

be a sequence of nested domains. Except Ω_0 has to be a rectangle, the remaining $\Omega_k \in \mathbb{R}^2, k = 1,\ldots,N$ represents the region selected to be refined at level k and its boundary $\partial\Omega_k$ is aligned with the edges of Δ^{k-1}. The union of all the grid line segments of Δ^k that lie in $\Omega_k, k = 0,1,\ldots,N$ is referred to as a hierarchical triangular mesh. A hierarchical triangular mesh divides the domain Ω_0 into a hierarchical triangular partition, denoted by D^N. Obviously,

$$D^0 \subseteq D^1 \subseteq \cdots \subseteq D^N,$$

with $D^0 = \Delta^0$. Our goal is to define hierarchical spline spaces over D^N.

Fig. 5(a) shows a nested sequence of type-II triangular partitions of domain $\Omega_0 : \Delta^0 \not\subseteq \Delta^1 \not\subseteq \Delta^2$, over which a nested sequence of spline spaces is defined: $S^0 \not\subseteq S^1 \not\subseteq S^2$. Fig. 5(b) shows a nested sequence of domains $\Omega_0 = \Omega_1 \supseteq \Omega_2$, together with the corresponding type-II hierarchial mesh, where $\Omega_0 = \Omega_1$ is the red rectangular domain and Ω_2 is the interior of the polygon marked with blue line segments. The corresponding hierarchical type-II triangular partition D^2 is illustrated in Fig. 5(c) (while $D^0 = \Delta^0, D^1 = \Delta^1$).

Finally, the support of a function f is defined as

$$\operatorname{supp} f = \{\mathbf{x} : f(\mathbf{x}) \neq 0 \wedge \mathbf{x} \in \Omega_0\}.$$

4.2. Hierarchical bivariate splines

Now we can define the hierarchical spline basis functions on a hierarchical triangular partition.

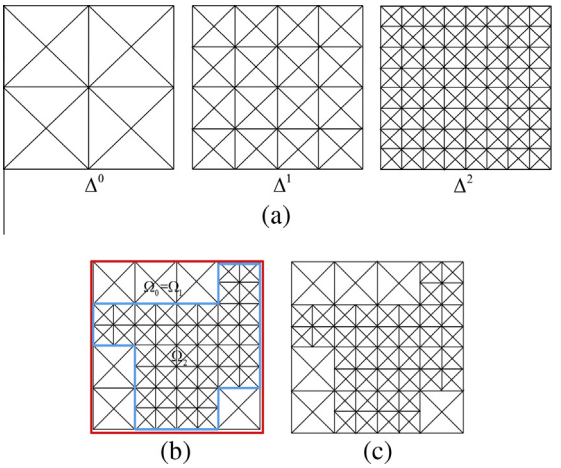

Fig. 5. (a) nested type-II triangular partition: $\Delta^0 \subsetneq \Delta^1 \subsetneq \Delta^2$. (b) Nested domains: $\Omega_0 \supseteq \Omega_1 \supseteq \Omega_2$, together with the hierarchical mesh. (c) Hierarchical type-II triangular partition D^2, while $D^0 = \Delta^0$ and $D^1 = \Delta^1$.

Definition 1. Let $\mathcal{B}^k$ be a basis of the spline space S^k defined on a regular triangular partition Δ^k of domain $\Omega_0, k = 0, 1 \ldots, N$, with $\Delta^0 \subsetneq \Delta^1 \subsetneq \cdots \subsetneq \Delta^N$. The hierarchical bivariate spline basis $\mathcal{H}$ is recursively constructed as follows.

1. Initialization: $\mathcal{H}^0 = \{\beta \in \mathcal{B}^0 : \text{supp}\beta \neq \emptyset\}$.
2. Recursive case: $\mathcal{H}^{l+1} = \mathcal{H}_A^{l+1} \cup \mathcal{H}_B^{l+1}$, for $l = 0, \ldots, N-1$, where

   $$\mathcal{H}_A^{l+1} = \{\beta \in \mathcal{H}^l : \text{supp } \beta \subsetneq \Omega_{l+1}\},$$

   and

   $$\mathcal{H}_B^{l+1} = \{\beta \in \mathcal{B}^{l+1} : \text{supp } \beta \subsetneq \Omega_{l+1}\}.$$
3. $\mathcal{H} = \mathcal{H}^N$.

As an illustration, we explain how to construct hierarchical bivariate spline basis $\mathcal{H}$ for hierarchical spline space $H_2^1(D^2)$, where D^2 is the hierarchical type-II triangular partition defined in Fig. 5. For convenience, we mark the central vertex of the support of a basis function in $S_2^1(\Delta_{mn}^{(2)})$ with a sold circle to represent the basis function as shown in Fig. 6(a) and (b) illustrates all the linearly independent basis functions in $\mathcal{B}^1$ defined by Eq. (4) which spans spline space $S_2^1(\Delta^1)$, where $\Delta^1 = \Delta_{mn}^{(2)}$ with $m = n = 4$.

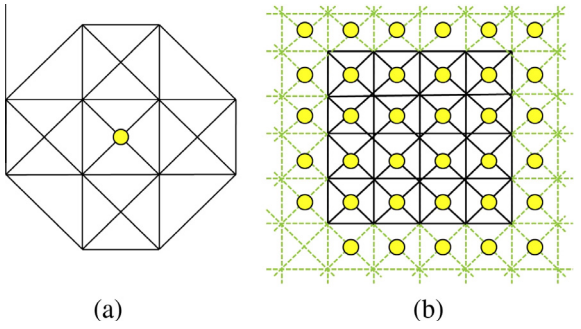

Fig. 6. (a) The center of the support of a basis function in $S_2^1(\Delta_{mn}^{(2)})$ is marked with a yellow circle. (b) The basis functions of $S_2^1(\Delta_{mn}^{(2)})$ defined by Eq. (4) are represented by circles. (For interpretation of the references to color in this figure legend, the reader is referred to the web version of this article.)

Because $\Omega_0 = \Omega_1$, so $\mathcal{H}^1 = \mathcal{B}^1$, thus $\mathcal{H} = \mathcal{H}^2$ are composed of two parts: $\beta \in \mathcal{B}^1, \text{supp } \beta \subsetneq \Omega_2$ and $\beta \in \mathcal{B}^2, \text{supp } \beta \subsetneq \Omega_2$. The first part and second part are represented by yellow solid circles in Fig. 7(a) and (b) respectively. Notice that there are 9 basis functions in $\mathcal{B}^1$ which are not included in the first part. On the other hand, the 11 yellow circles outside of the domain Ω_0 in Fig. 7(b) should be included in the second part, which are easy to be neglected.

4.3. Properties

Now we discuss some properties of the bivariate hierarchical splines constructed in the above subsection.

Theorem 3. *The bivariate hierarchical spline basis $\mathcal{H}$ constructed in Section 4.2 have the following properties:*

1. Nonnegativity: $\beta \geqslant 0, \forall \beta \in \mathcal{H}$.
2. Compact support: $\beta \in \mathcal{H}$ has compact support.
3. Polynomial completeness: $\mathbb{P}_2 \subset H_2^1(D)$ for hierarchical type-II triangular partition D, and $\mathbb{P}_1 \subset H_3^1(D)$ for hierarchical type-I triangular partition D.
4. Linear independency: the functions in $\mathcal{H}$ are linearly independent.
5. Nested property: $span\mathcal{H}^k \subset span\mathcal{H}^{k+1}, k = 0, 1, \ldots, N-1$.

Proof. The first three properties are obvious. The linear independency and nested property are proved in Lemmas 4 and 5. □

Lemma 4. *The functions in $\mathcal{H}$ are linearly independent.*

Proof. We have to prove that

$$\sum_{\beta \in \mathcal{H}} c_\beta \beta = 0 \Rightarrow c_\beta = 0, \quad \textit{for all } \beta. \tag{5}$$

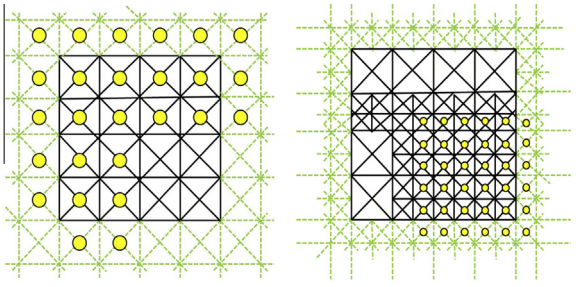

Fig. 7. Basis of hierarchical spline space $H_2^1(D^2)$.

The sum $\sum_{\beta\in\mathcal{H}} c_\beta\beta = 0$ can be rearranged as

$$\sum_{\beta\in\mathcal{H}\cap\mathcal{B}^0} c_\beta\beta + \sum_{\beta\in\mathcal{H}\cap\mathcal{B}^1} c_\beta\beta + \cdots \sum_{\beta\in\mathcal{H}\cap\mathcal{B}^N} c_\beta\beta = 0.$$

Since the functions in $\mathcal{H}\cap\mathcal{B}^0$ are a subset of $\mathcal{B}^0$, they are linearly independent. Only these functions are non-zero on $\Omega_0\setminus\Omega_1$, hence, in view of their local linear independence, we conclude that $c_\beta = 0$ for $\beta\in\mathcal{H}\cap\mathcal{B}^0$.

Analogously, when we consider the remaining sums in the sequence, firstly we know that the functions in $\mathcal{H}\cap\mathcal{B}^k$ are linearly independent since $\mathcal{H}\cap\mathcal{B}^k \not\subseteq \mathcal{B}^k, k = 1,\ldots N$. Then, except for the functions already considered in the previous sums, namely $\beta\in\mathcal{H}\cap\mathcal{B}^0,\ldots,\beta\in\mathcal{H}\cap\mathcal{B}^{k-1}$, only the functions in $\mathcal{H}\cap\mathcal{B}^k$ are non-zero on $\Omega_k\setminus\Omega_{k+1}$. This implies that $c_\beta = 0$ for $\beta\in\mathcal{H}\cap\mathcal{B}^k$ with $k = 1,\ldots N$. The lemma is thus proved. □

Lemma 5. We have

$$span\mathcal{H}^k \subset span\mathcal{H}^{k+1}, k = 0,1,\ldots,N-1.$$

Proof. Any $f\in span\mathcal{H}^k$ can be expressed as

$$f = \sum_{\beta\in\mathcal{H}^k} d_\beta(f)\beta = \sum_{\substack{\beta\in\mathcal{H}^k\\ supp\beta\not\subseteq\Omega_{k+1}}} d_\beta(f)\beta + \sum_{\substack{\beta\in\mathcal{H}^k\\ supp\beta\subseteq\Omega_{k+1}}} d_\beta(f)\beta. \tag{6}$$

The first sum in the right-hand side of the above relation Eq. (6) collects all basis functions in $\mathcal{H}_A^{k+1}$. In view of the nested nature of the underlying spaces $\mathcal{B}^k, k = 0,\ldots,N$, we can express each basis function $\beta\in\mathcal{H}^k$ as linear combination of basis functions which belong to $\mathcal{B}^{k+1}$, so we have

$$\begin{aligned} f &= \sum_{\beta\in\mathcal{H}_A^{k+1}} d_\beta(f)\beta + \sum_{\substack{\beta\in\mathcal{H}^k\\ supp\beta\not\subseteq\Omega_{k+1}}} d_\beta(f)\left(\sum_{\substack{\alpha\in\mathcal{B}^{k+1}\\ supp\alpha\subseteq\Omega_{k+1}}} c_\alpha^{k+1}\alpha\right)\\ &= \sum_{\beta\in\mathcal{H}_A^{k+1}} d_\beta(f)\beta + \sum_{\substack{\alpha\in\mathcal{B}^{k+1}\\ supp\alpha\not\subseteq\Omega_{k+1}}}\left(\sum_{\substack{\beta\in\mathcal{H}^k\\ supp\beta\not\subseteq\Omega_{k+1}}} c_\alpha^{k+1} d_\beta(f)\right)\alpha\\ &= \sum_{\beta\in\mathcal{H}_A^{k+1}} d_\beta(f)\beta + \sum_{\alpha\in\mathcal{H}_B^{k+1}} d_\alpha(f)\alpha. \end{aligned}$$

Hence, $f\in span\mathcal{H}^{k+1}$. □

Remark 1. The hierarchical B-spline space $H_k^\mu(D)$ has global continuity μ for any hierarchical triangular partition D, so it does not lose continuity order at hanging nodes of D.

After defining a basis for a hierarchical spline space, one can define a hierarchical spline surface as

$$\mathbf{S}(x,y) = \sum_{\beta\in\mathcal{H}} \mathbf{P}_\beta\beta(x,y), \quad (x,y)\in\Omega_0, \tag{7}$$

where $\mathbf{P}_\beta\in\mathbb{R}^3$ are the control points, and $\beta(x,y), \beta\in\mathcal{H}$ are basis functions. Ω_0 is a 2D rectangular parametric domain.

5. Surface fitting

In this section, we show applications of hierarchical splines on regular triangular partitions in surface fitting. The hierarchial spline spaces H_2^1 and H_3^1 are chosen for illustration. Here H_2^1 is defined on hierarchical type-II triangular partitions, and H_3^1 is defined on hierarchical type-I triangular partitions. Comparisons are made with hierarchical tensor product counterparts – $H_{2,2}^{1,1}$ and $H_{3,3}^{1,1}$ respectively. Here $H_{2,2}^{1,1}$ stands for C^1 continuous biquadratic hierarchical spline space which is constructed from C^1 continuous uniform biquadratic splines $S_{2,2}^{1,1}$. Similarly, hierarchical bicubic spline space $H_{3,3}^{1,1}$ is constructed from uniform bicubic spline space $S_{3,3}^{1,1}$. The reader is referred to [4] for details.

Suppose we are given an open mesh model with vertices $\mathbf{P}_i$, $i = 1,2,\ldots,N$ in 3D space, and their corresponding parameter values $(s_i,t_i), i = 1,2,\ldots,N$ obtained from some parametrization of the mesh (we use the parameterization method in [15] in the current paper). The parameter domain is assumed to be $\Omega_0 = [0,1]\times[0,1]$. We are going to find a hierarchical spline surface $\mathbf{S}(s,t)$ to approximate the mesh model.

The surface fitting scheme repeats the following step 2 and 3 until the approximation error is satisfied with respect to a given tolerance ε.

1. Construct a uniform (triangular or rectangular) partition T_0 of Ω_0. T_0 is the initial mesh. Set $k = 0$.
2. Compute a least-squares approximation $\mathbf{S}(s,t)$ by minimizing:
$$\sum_{i=1}^{N}(\mathbf{S}(s_i,t_i) - \mathbf{P}_i)^2$$
according to current hierarchical spline space $\mathcal{H}^k$. The underlying hierarchical mesh is denoted by T_k.
3. Search for the violated cells in T_k. Then split these cells into four sub-cells to obtain a new mesh T_{k+1}. A violated cell is the cell over which the fitting error is greater than ε. The fitting error over a cell θ is calculated as the maximum of $\|\mathbf{P}_i - \mathbf{S}(s_i,t_i)\|_2$ for the points $(s_i,t_i)\in\theta$. Set $k := k+1$.

We demonstrate three examples to illustrate the above algorithm. The approximate error of a model is defined as the maximum of $\|\mathbf{P}_i - \mathbf{S}(s_i,t_i)\|_2, i = 1,\ldots,N$.

Example 1. Consider a piecewise quadratic function

$$f(x,y) = \begin{cases} (x-y)^2, & x\leqslant y\\ -(x-y)^2, & \text{else}\end{cases}$$

We approximate $f(x,y)$ by a hierarchical spline function from H_2^1, and a tensor product hierarchical spline function from $H_{2,2}^{1,1}$.

By sampling data points of $f(x,y)$ on a 51×51 uniform grid defined on the domain $[0,1]\times[0,1]$, we obtain two

approximated functions $g_1(x,y)$ and $g_2(x,y)$ respectively from H_2^1 and $H_{2,2}^{1,1}$, as shown in Fig. 8.

$g_1(x,y) \in H_2^1$ has 15 degrees of freedom (DOF for short) with an approximation error 3.0×10^{-8}, while $g_2(x,y)$ has 638 DOF with an approximation error 9.7×10^{-5}. The reason why H_2^1 approximates better in this example is that, $g_1(x,y)$ can naturally capture the second order derivative discontinuity of $f(x,y)$ along the diagonal line $y = x$.

Example 2. We consider the fitting of a 3D mesh model – a female head with 19,231 points and 38,388 faces.

We start from a uniform type-II triangular partition $\Delta_{88}^{(2)}$ (for H_2^1) or a uniform 8×8 tensor product partition (for $H_{2,2}^{1,1}$). The surfaces at various levels approximated by spline spaces H_2^1 and $H_{2,2}^{1,1}$ are shown in Fig. 15(a) and (b) respectively. Table 1 summarizes the fitting results. From the statistic data, the approximation surfaces by two spline spaces H_2^1 and $H_{2,2}^{1,1}$ have about the same approximation error at the same level, but H_2^1 needs only about half of DOF compared with $H_{2,2}^{1,1}$.

Example 3. In this example, we fit Lauransana model with surfaces from H_3^1 and $H_{3,3}^{1,1}$. The model has 6301 points and 12,487 faces.

The initial partition used for $H_3^1(H_{3,3}^{1,1})$ is a uniform type-I triangular partition $\Delta_{88}^{(1)}$(uniform 8×8 tensor product partition). The surfaces approximated by spline spaces H_3^1 and $H_{3,3}^{1,1}$ are shown in Fig. 9(a) and (b) respectively. Table 2 summarizes the fitting results. From the statistic data, the approximation error by H_3^1 is a little larger than that by $H_{3,3}^{1,1}$, but with a smaller number of DOFs.

6. Solving elliptic PDEs

In this section, we discuss how to use hierarchical bivariate B-splines defined in Section 4.2 to solve elliptic PDEs with Dirichlet boundary constraint. Due to the boundary constraint, the spline space $S_2^1(\Delta_{mn}^{(2)})$ cannot be used directly, so we firstly introduce a subspace $S_2^{1,0}(\Delta_{mn}^{(2)})$ which satisfies the boundary constraint. The hierarchical

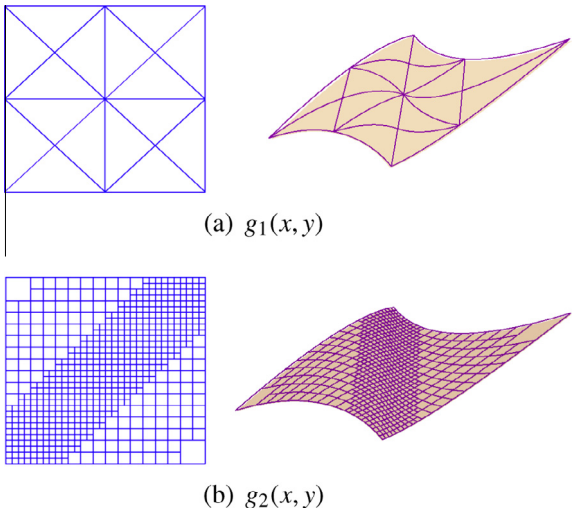

Fig. 8. Two approximated functions of Example 1. The curves on the right surfaces are the images of the left underlying meshes.

Table 1
Statistic data for fitting Female Head model with $\#Points = 19,231$, $\#Faces = 38,388$.

Levels	H_2^1		$H_{2,2}^{1,1}$	
	DOF	Max error	DOF	Max error
0	99	0.597346	100	0.730179
1	208	0.403546	310	0.40666
2	321	0.37169	537	0.375345
3	505	0.33654	796	0.340688
4	769	0.32103	1198	0.322405
5	1070	0.26588	1699	0.264722
6	1459	0.204522	2397	0.205273
7	1877	0.132439	3165	0.143232
8	2161	0.0581819	3804	0.0666729
9	2336	0.048414	4195	0.0489152
10	2403	0.0333915	44,443	0.03445

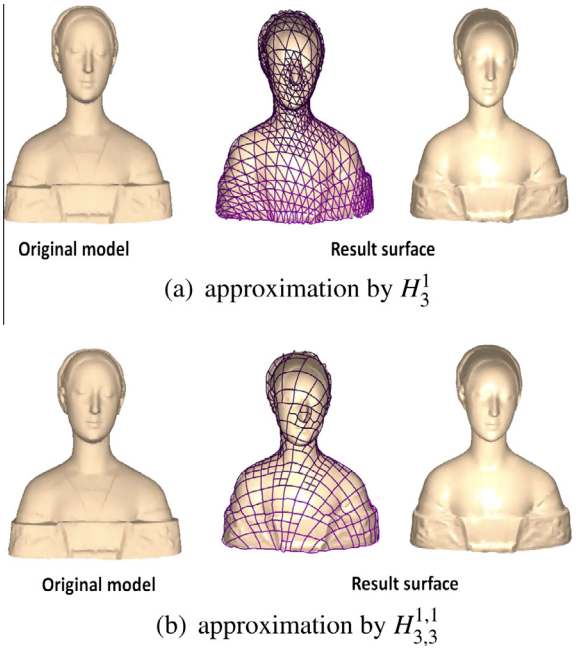

Fig. 9. Fitting Lauransana model in Example 3 with hierarchical spline spaces H_3^1 and $H_{3,3}^{1,1}$. The left column is the original surfaces and the right columns are approximation surfaces with hierarchical mesh.

Table 2
Statistic data for fitting Lauransana model with $\#Points = 6301$, $\#Faces = 12,487$.

Levels	H_3^1		$H_{3,3}^{1,1}$	
	DOF	Max error	DOF	Max error
0	195	0.358897	324	0.40361
1	628	0.34233	788	0.411683
2	776	0.311991	1028	0.314497
3	838	0.148043	1120	0.127306
4	926	0.0623309	1200	0.0422704
5	1066	0.0374738	1332	0.0269059

spline space $H_2^{1,0}$ can be constructed from $S_2^{1,0}(\Delta_{mn}^{(2)})$ by the process in Section 4.2. We compare our results with finite element function space – C^1 continuous hierarchical tensor product spline space $H_{2,2}^{1,1}$ constructed from C^1 continuous biquadratic spline space $S_{2,2}^{1,1}$. From the numerical results, it suggests that the hierarchical spline spaces $H_2^{1,0}$ and $H_{2,2}^{1,1}$ have similar convergence rate, and they are superior to uniform spline spaces $S_2^{1,0}(\Delta_{mn}^{(2)})$ and $S_{2,2}^{1,1}$.

6.1. Model problem

The elliptic model problem we considered is a Poisson's equation defined on a two-dimensional rectangle domain $\Omega = [0,1] \times [0,1]$ with Dirichlet boundary Γ, which is defined as follows:

$$\begin{aligned} &-\Delta u = f \text{ on } \Omega \\ &u = 0 \text{ on } \Gamma \end{aligned} \tag{8}$$

where $f \in L^2(\Omega)$.

The weak form solution of problem Eq. (8) is to seek $u \in V$ such that

$$a(u,v) = F(v), \quad \forall v \in V, \tag{9}$$

where a is the bilinear form and F is the linear functional defined by

$$\begin{aligned} a(u,v) &= \int_\Omega \nabla u \cdot \nabla v d\Omega, \\ F(v) &= \int_\Omega f v d\Omega. \end{aligned} \tag{10}$$

The trial and test space V is the usual Sobolev space $H^1(\Omega)$ vanishing at the boundary Γ, that is

$$V = \{v \in H^1(\Omega) : v = 0 \text{ on } \Gamma\}.$$

The energy norm associated with the bilinear form is defined by

$$\|v\|_E = \sqrt{a(v,v)}. \tag{11}$$

6.2. Hierarchical spline space $H_2^{1,0}$

Let $B(x,y)$ be the basis function defined in Fig. 4(a) and B_{ij} be the translation of $B(x,y)$:

$$B_{ij}(x,y) = B(mx - i + 1/2, nx - j + 1/2),$$

then the set

$$\mathcal{B} = \{B_{ij}(x,y) | i = 0, \ldots, m+1, j = 0, \ldots, n+1\}$$

spans the spline space $S_2^1(\Delta_{mn}^{(2)})$.

The spline space $S_2^{1,0}(\Delta_{mn}^{(2)})$ is defined as follows [16]:

$$\begin{aligned} S_2^{1,0}(\Delta_{mn}^{(2)}) = \{&s \in S_2^1(\Delta_{mn}^{(2)}) : s(0,\cdot) = 0, \\ &s(1,\cdot) = 0, s(\cdot,0) = 0, s(\cdot,1) = 0\}. \end{aligned} \tag{12}$$

The basis functions of $S_2^{1,0}(\Delta_{mn}^{(2)})$ can be constructed by linear combination of B_{ij}. Specifically, let $\widetilde{B}_{i,j}(x,y) \in S_2^{1,0}(\Delta_{mn}^{(2)})$, then we have

$$\begin{cases} \widetilde{B}_{1,1}(x,y) = B_{1,1}(x,y) - B_{0,1}(x,y) - B_{1,0}(x,y) + B_{0,0}(x,y), \\ \widetilde{B}_{m,1}(x,y) = B_{m,1}(x,y) - B_{m+1,1}(x,y) - B_{m,0}(x,y) + B_{m+1,0}(x,y), \\ \widetilde{B}_{1,n}(x,y) = B_{1,n}(x,y) - B_{0,n}(x,y) - B_{1,n+1}(x,y) + B_{0,n+1}(x,y), \\ \widetilde{B}_{m,n}(x,y) = B_{m,n}(x,y) - B_{m,n+1}(x,y) - B_{m+1,n}(x,y) + B_{m+1,n+1}(x,y), \end{cases} \tag{13}$$

$$\begin{cases} \widetilde{B}_{i,1}(x,y) = B_{i,1}(x,y) - B_{i,0}(x,y), \quad i = 2,3,\ldots,m-1, \\ \widetilde{B}_{i,n}(x,y) = B_{i,n}(x,y) - B_{i,n+1}(x,y), \quad i = 2,3,\ldots,m-1, \\ \widetilde{B}_{1,j}(x,y) = B_{1,j}(x,y) - B_{0,j}(x,y), \quad j = 2,3,\ldots,n-1, \\ \widetilde{B}_{m,j}(x,y) = B_{m,j}(x,y) - B_{m+1,j}(x,y), \quad j = 2,3,\ldots,n-1, \end{cases} \tag{14}$$

$$\begin{aligned} \widetilde{B}_{i,j}(x,y) = B_{i,j}(x,y) \quad & i = 2,3,\ldots,m-1, \\ & j = 2,3,\ldots,n-1. \end{aligned} \tag{15}$$

The basis functions defined by formula Eqs. (13)–(15) are called corner spline, edge spline and interior spline of $S_2^{1,0}(\Delta_{mn}^{(2)})$ respectively. The supports of these three kinds of splines are shown in Fig. 10. One can show that the dimension of space $S_2^{1,0}(\Delta_{mn}^{(2)})$ is

$$dim S_2^{1,0}(\Delta_{mn}^{(2)}) = mn - 1.$$

The following set of functions forms a basis of $S_2^{1,0}(\Delta_{mn}^{(2)})$:

$$\widetilde{\mathcal{B}} = \{\widetilde{B}_{ij} : 1 \leqslant i \leqslant m, 1 \leqslant j \leqslant n, (i,j) \neq (i_0,j_0)\},$$

where (i_0,j_0) is a specified index, $i_0 \in [1,m], j_0 \in [1,n]$.

The hierarchical spline space $H_2^{1,0}$ corresponding to $S_2^{1,0}(\Delta_{mn}^{(2)})$ is defined as in Definition 1. Similarly, one can define its tensor product counterpart $H_{2,2}^{1,1}$.

6.3. Finite element discretization

Now we are ready to use hierarchical spline space $H_2^{1,0}$ and $H_{2,2}^{1,1}$ to solve elliptic problem Eq. (9). For simplicity, we simply use $\mathcal{H}$ to stand for $H_2^{1,0}$ or $H_{2,2}^{1,1}$. The finite element approximation of problem Eq. (9) with $\mathcal{H}$ means to find a function $u_h \in \mathcal{H}$ such that

$$a(u_h, v) = F(v) \tag{16}$$

for all test functions $v_h \in \mathcal{H} \subset V$.

Suppose $\mathcal{H} = \{\beta_i\}_{i=1}^n, u_h = \sum_{i=1}^n c_i \beta_i$, then problem Eq. (16) is turned into solving the following linear equation

$$LC = B,$$

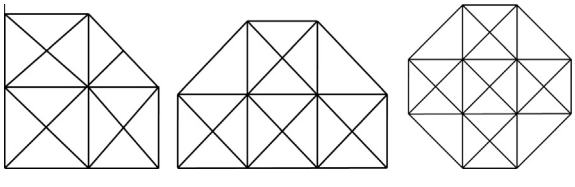

Fig. 10. From left to right: the supports of corner spline, edge spline and interior spline of $S_2^{1,0}(\Delta_{mn}^{(2)})$.

Table 3
Computational results by $H_2^{1,0}$ for Example 4 under uniform global refinement.

DOF	$\|u-u_h\|_{L^2}$	CR	$\|u-u_h\|_E$	CR
3	2.14789e−3		2.54794e−2	
15	1.89944e−4	3.0141	5.46014e−3	1.9142
63	2.08673e−5	3.0779	1.30255e−3	1.9973
255	2.51227e−6	3.0283	3.21580e−4	2.0010
1023	3.10966e−7	3.0078	8.01381e−5	2.0004
4095	3.87764e−8	3.0019	2.00185e−5	2.0001

where L is a $n\times n$ matrix with the element $L(i,j)=a(\beta_i,\beta_j)$, B is a $n\times 1$ vector with element $B(i)=F(\beta_i)$ and $C=(c_1,\ldots,c_n)^T$.

All the numerical experiments are tested over a domain $\Omega=[0,1]\times[0,1]$. The refinement at each level is achieved by performing the marking strategy used in [17] with a parameter θ, which is used to control the refinement process [18]. The refinement strategy is based on an error estimate on a cell. Here we use the residual-based posteriori error estimate η_K on a cell K of mesh, defined by

$$\eta_K^2=h_k^2\|\Delta u+f\|_{L^2(K)}^2,$$

where h_K is the diameter of cell K. The posterior error on mesh $\mathcal{T}$ is the sum of η_K on each cell, that is

$$\eta_{\mathcal{T}}=\left(\sum_{K\in\mathcal{T}}\eta_K^2\right)^{1/2}.$$

The convergence rate CR with respect to the norm $\|\cdot\|$ at the refinement level k is roughly computed by

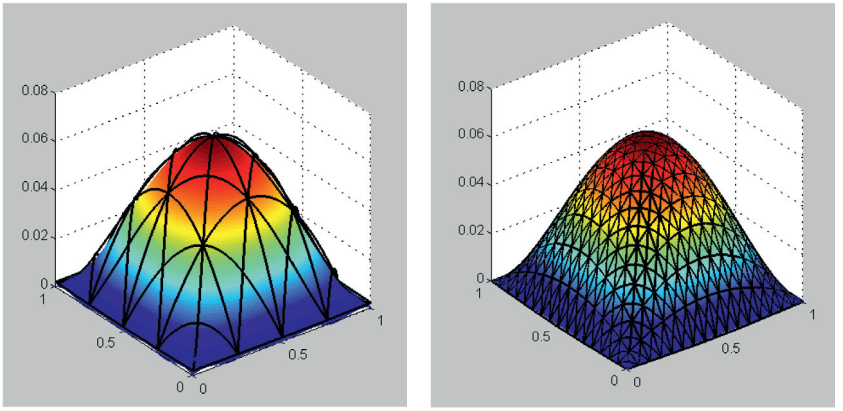

(a) $DOF = 15$ (b) $DOF = 255$

Fig. 11. Discrete solutions u_h by $H_2^{1,0}$ of Example 4.

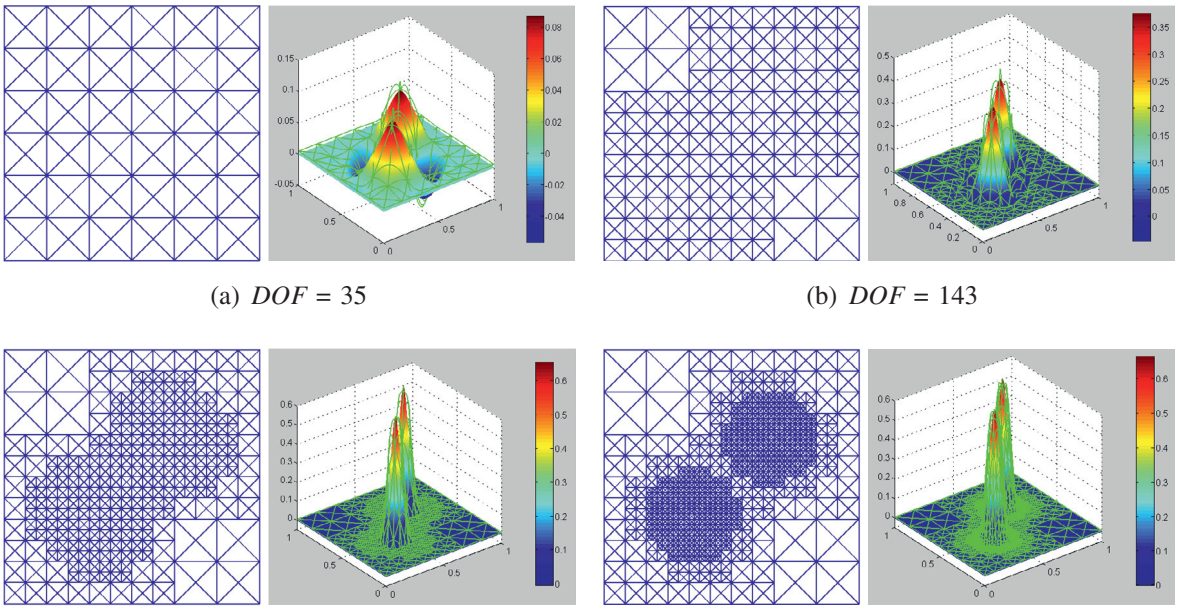

(a) $DOF = 35$ (b) $DOF = 143$

(c) $DOF = 279$ (d) $DOF = 545$

Fig. 12. Discrete solutions u_h of Example 5 solved with $H_2^{1,0}$. The green curves on the surfaces are the images of the hierarchical meshes. (For interpretation of the references to color in this figure legend, the reader is referred to the web version of this article.)

$$CR = \frac{2log(\|e_{h,k-1}\|/\|e_{h,k}\|)}{log(n_k/n_{k-1})},$$

where n_k is the degree of freedom at level k and $e_{h,k}$ denotes the error (energy-norm error $\|u-u_h\|_E$ or L^2-norm error $\|u-u_h\|_{L^2}$) at level k. For convenience, we use DOF as the abbreviation for degree of freedom (=number of basis functions).

In the following, we provide several numerical examples to illustrate the numerical property of hierarchical spline space $H_2^{1,0}$, together with comparisons with that of spline spaces $H_{2,2}^{1,1}$, $S_2^{1,0}$ and $S_{2,2}^{1,1}$.

Example 4. In this experiment, the global uniform refinement is performed. The exact solution is $u(x,y) = e^{x(1-x)y(1-y)} - 1$ and f is determined by Eq. (8).

The computational results for spline space $H_2^{1,0}$ under 6 different resolutions, i.e. $\Delta_{mn}^{(2)}$ with $m = n = 2, 4, 8, 16, 32, 64$, are shown in Table 3. From the results, the convergence rate CR with respect to L^2-norm (energy-norm) is about three (two), which is consistent with the theory of finite element. Fig. 11 depicts two numerical solutions.

Example 5. In this example, the exact solution is

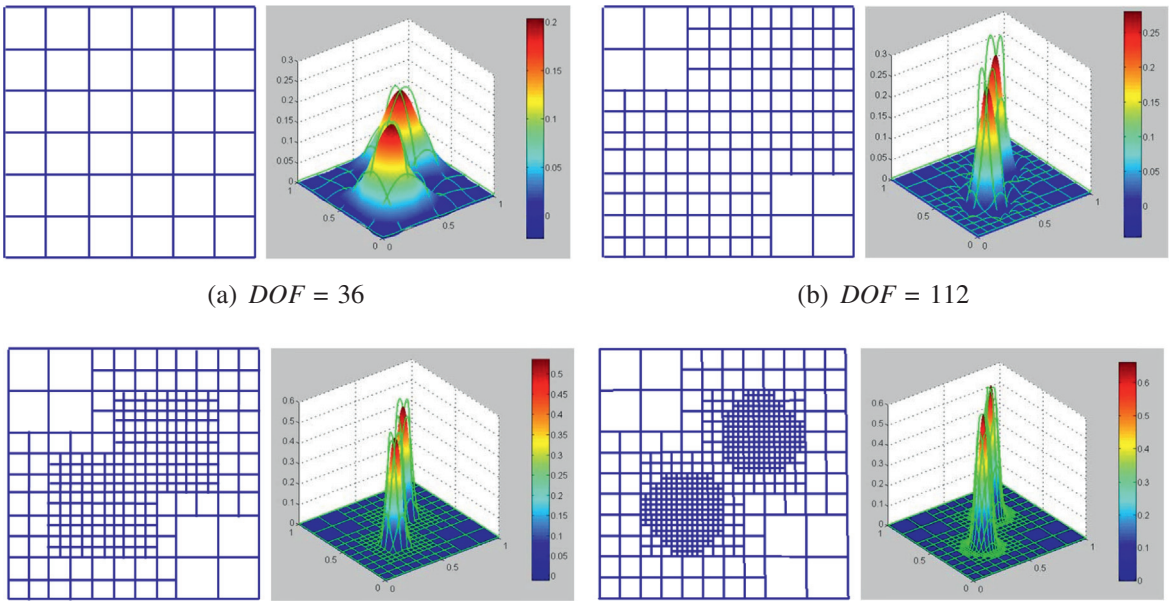

(a) $DOF = 36$ (b) $DOF = 112$

(c) $DOF = 218$ (d) $DOF = 460$

Fig. 13. Discrete solutions u_h of Example 5 solved by $H_{2,2}^{1,1}$. The green curves on the surfaces are the images of the hierarchical meshes. (For interpretation of the references to color in this figure legend, the reader is referred to the web version of this article.)

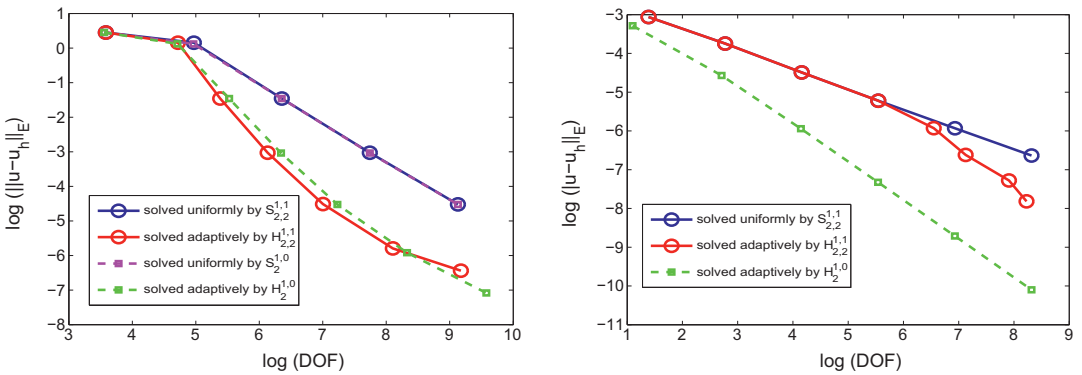

(a) Example 5 (b) Example 6

Fig. 14. Convergence plot for Examples 5 and 6.

$$u(x,y) = \frac{2.0}{3.0exp((20x-13)^2+(20y-13)^2)} + \frac{2.0}{3.0exp((20x-7)^2+(20y-7)^2)},$$

and f is determined by Eq. (8).

The exact solution $u(x,y)$ has two peaks and it decays very fast away from the two peaks. For the two hierarchical spline spaces $H_2^{1,0}$ and $H_{2,2}^{1,1}$, Figs. 12 and 13 depict respectively the numerical solutions (right) and the corresponding refined meshes (left) at the first four levels. It is worth noting that the numerical solutions quickly

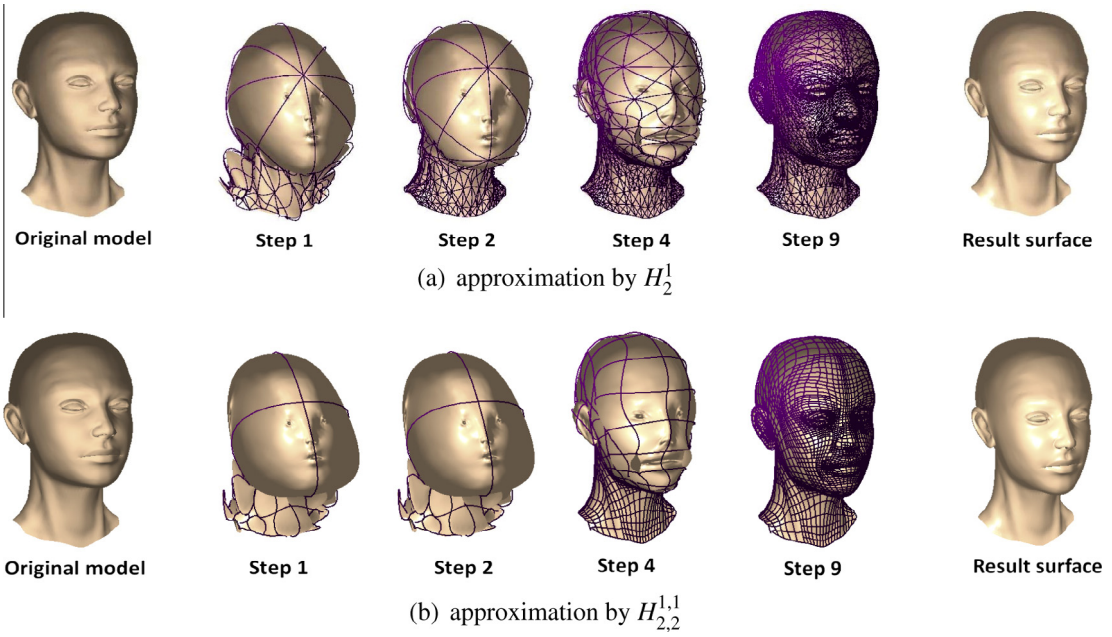

Fig. 15. Fitting Female Head model in Example 2 with hierarchical spline spaces H_2^1 and $H_{2,2}^{1,1}$. The left column is the original surfaces and the right columns are approximation surfaces with hierarchical meshes.

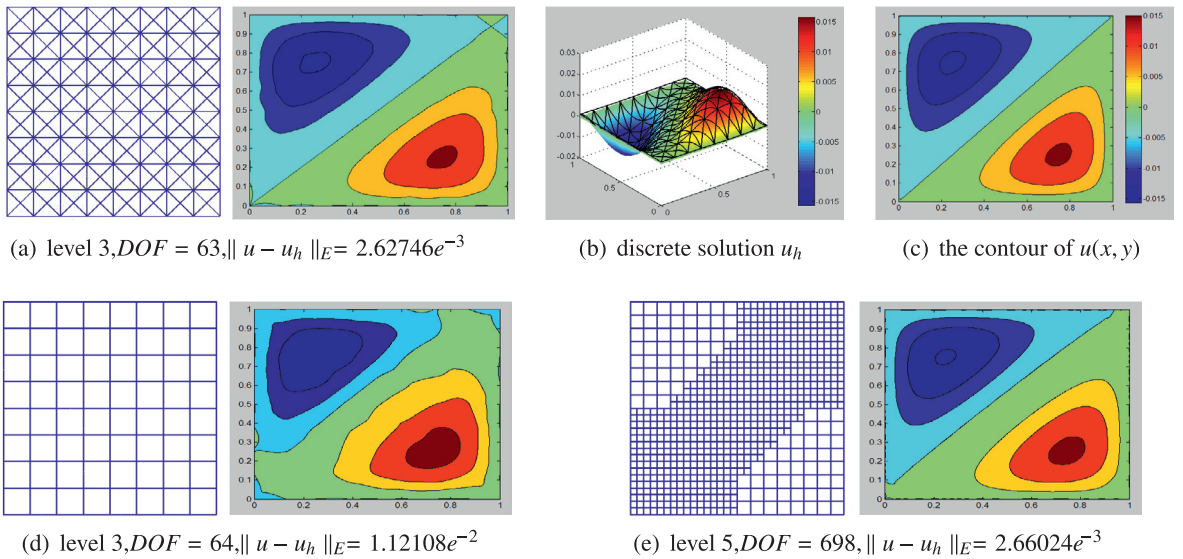

Fig. 16. The refined meshes (left) and the contours of the corresponding discrete solutions (right) for Example 6; (a) is solved by $H_2^{1,0}$ and (d) and (e) are solved by $H_{2,2}^{1,1}$.

capture the two peaks as the refinement proceeds. The energy-norm errors with respect to DOF are plotted in Fig. 14(a). From the numerical results, both $H_2^{1,0}$ and $H_{2,2}^{1,1}$ have about the same convergence rate, which is faster than the uniform refinement splines.

Example 6. In the final example, the exact solution is

$$u(x,y) = \begin{cases} (x-y)(x-y)(1-x)y, & x > y \\ -(x-y)(x-y)(1-y)x, & x \leqslant y \end{cases}$$

and f is determined by Eq. (8).

For this example, the initial mesh is $\Delta_{mn}^{(2)}$ with $m = n = 2$ when it is solved by $H_2^{1,0}$. Fig. 16(a) shows the refined mesh and the contour of the corresponding solution at the third level. The corresponding discrete solution u_h is shown in Fig. 16(b). The contour of exact solution $u(x,y)$ is shown in Fig. 16(c).

Fig. 16(d) shows the results at the third level solved by $H_{2,2}^{1,1}$. From the contour plot, it can be seen that the solution by $H_{2,2}^{1,1}$ is much less accurate than that by $H_2^{1,0}$ at the same level. Fig. 16(e) depicts the results at the level five solved by $H_{2,2}^{1,1}$, where the energy-error has the same magnitude as the one in Fig. 16(a), while the DOF is much larger than the one used by $H_2^{1,0}$ at the level three. Furthermore, $H_2^{1,0}$ has a much faster convergence rate than $H_{2,2}^{1,1}$, as shown in Fig. 14(b). The reason why H_2^1 approximates better in this example is similar to the analysis in Example 1, namely H_2^1 can naturally capture the second order derivative discontinuity of $u(x,y)$ along the diagonal line $y = x$.

Remark 2. Notice that here we do not consider the boundary element basis for the spline space $S_3^1(\Delta_{mn}^{(1)})$, since there should be at least one so-called 'global' spline function which is not easy to be constructed (see the theory in Section 2.6 of [2]).

7. Conclusion

In this paper, we extend the hierarchical paradigm of tensor-product B-splines to bivariate splines defined on regular triangular partitions and propose a method to construct basis functions of such a hierarchical spline space. The basis functions constructed have nice properties such as, nonnegativity, compact support, linear independence and nested property. The spline space spanned by these basis functions supports local refinement, which is important in adaptive geometric modeling and adaptive finite element. We illustrate applications of such splines in geometric modeling and solving numerical PDEs, and the results suggest that hierarchical B-splines defined on regular triangular partitions seem promising in applications.

There are a few problems worthy of further investigation. First, there is a natural spline space $S_k^\mu(D)$ which consists of all the piecewise polynomials of degree k with the order of smoothness μ defined over a hierarchical triangular partition D. Obviously, our hierarchical spline space $H_k^\mu(D)$ defined in this paper is a subset of $S_k^\mu(D)$. The question is what is the relationship between these two spline spaces? What is the dimension of the spline space $S_k^\mu(D)$ for a hierarchical triangular partition? Second, how to extend our hierarchical splines to spline spaces defined on other types of triangular partitions? Finally, we will investigate further applications of these hierarchical splines in iso-geometric analysis and geometric modeling.

Acknowledgments

The authors thank the reviewers for providing useful comments and suggestion. The work is supported by 973 Program 2011CB302400, the NSF of China No. 11031007.

References

[1] D. Forsey, R. Bartels, Hierarchical B-spline refinement, Comp. Graph. 22 (1988) 205–212.
[2] R. Wang, Multivariate Splines and its Application, Science Publisher, China, 1994.
[3] R. Kraft, Adaptive and linearly independent multilevel B-splines, in: A.L. Méhauté, C. Rabut, L.L. Schumaker (Eds.), Surface Fitting and Multiresolution Methods, Vanderbilt University Press, Nashville, TN, 1997, pp. 209–218.
[4] A.-V. Vuong, C. Giannelli, B. Jüttler, B. Simeon, A hierarchical approach to adaptive local refinement in isogeometric analysis, Comput. Meth. Appl. Mech. Eng. 200 (2011) 3554–3567.
[5] C. Giannelli, B. Jüttler, H. Speleers, THB-splines: the truncated basis for hierarchical splines, Comp. Aided Geom. Des. 29 (2012) 485–498.
[6] T.W. Sederberg, J. Zheng, A. Bakenov, A. Nasri, T-splines and T-NURCCSs, ACM Trans. Graph. 22 (3) (2003) 477–484.
[7] T.W. Sederberg, D.L. Cardon, G.T. Finnigan, N.S. North, J. Zheng, T. Lyche, T-spline simplification and local refinement, ACM Trans. Graph. 23 (3) (2004) 276–283.
[8] M.A. Scott, X. Li, T.W. Sederberg, T.J.R. Hughes, Local refinement of analysis-suitable T-splines, Comp. Meth. Appl. Mech. Eng. 213–216 (2012) 206–222.
[9] J. Deng, F. Chen, X. Li, C. Hu, W. Tong, Z. Yang, Y. Feng, Polynomial splines over hierarchical T-meshes, Graph. Mod. 74 (2008) 76–86.
[10] T. Dokken, T. Lyche, K.F. Pettersen, Polynomial splines over locally refined box-partitions, Comp. Aided Geom. Des. 30 (2013) 331–356.
[11] M. Powell, M. Sabin, Piecewise quadratic approximations on triangles, ACM Trans. Math. Softw. 3 (1977) 316–325.
[12] H. Speleers, P. Dierckx, S. Vandewalle, Quasi-hierarchical Powell–Sabin B-splines, Comput. Aided Geom. Des. 26 (2009) 174–191.
[13] H. Speleers, C. Manni, F. Pelosi, M.L. Sampoli, Isogeometric analysis with Powell–Sabin splines for advection–diffusion–reaction problems, Comput. Meth. Appl. Mech. Eng. 221–222 (2012) 132–148.
[14] A. Yvart, S. Hahmann, G.-P. Bonneau, Hierarchical triangular splines, ACM Trans. Graph. 24 (2005) 1374–1391.
[15] M.S. Floater, Parameteriztion and smooth approximation of surface triangulations, Comp. Aided Geom. Des. 14 (1997) 231–250.
[16] K. Qu, Multivariate Splines and Some Application, Ph.D. thesis, Dalian University of Technology, 2010.
[17] A. Schmidt, K. Siebert, Design of Adaptive Finite Element Software: The Finite Element Toolbox ALBERTA, Springer, 2005.
[18] W. Döfler, A convergent adaptive algorithm for poisson's equation, SIAM J. Numer. Anal. 33 (1996) 1106–1124.